



## Sterol effect on interaction between amphidinol 3 and liposomal membrane as evidenced by surface plasmon resonance

Respati T. Swasono, Ryota Mouri, Nagy Morsy<sup>†</sup>, Nobuaki Matsumori, Tohru Oishi, Michio Murata<sup>\*</sup>

Department of Chemistry, Graduate School of Science, Osaka University, 1-1 Machikaneyama, Toyonaka, Osaka 560-0043, Japan

### ARTICLE INFO

#### Article history:

Received 23 December 2009

Revised 4 February 2010

Accepted 5 February 2010

Available online 10 February 2010

#### Keywords:

Amphidinol

Surface plasmon resonance

Cholesterol

Ergosterol

### ABSTRACT

The affinity of amphidinol 3 (AM3) to phospholipid membranes in the presence and absence of sterol was examined by surface plasmon resonance (SPR) experiments. The results showed that AM3 has 1000 and 5300 times higher affinity for cholesterol- and ergosterol-containing liposomes, respectively, than those without sterol. The two-state reaction model well reproduced the sensor grams, which indicated that the interaction is composed of two steps, which correspond to binding to the membrane and internalization to form stable complexes.

© 2010 Elsevier Ltd. All rights reserved.

A family of amphidinols (AMs) have been isolated as a potent antifungal agent from the marine dinoflagellates of genus *Amphidinium*.<sup>1–7</sup> AM homologues including luteophanols,<sup>8–10</sup> lingshuiols,<sup>11</sup> karatungliols,<sup>12</sup> amphezonol A<sup>13</sup> and carteraol E<sup>14</sup> have common structural features comprising a linear polyhydroxyl moiety, tetrahydropyran rings and an alkenyl chain of 14 or 16 carbon atoms. Unlike other natural or synthetic antifungal compounds, AMs lack nitrogenous polycycles or macrocycles in their structures. These unique features make AMs an interesting model to gain a better understanding of the molecular mechanism of antifungal action.

Since amphidinol 1 (AM1) was first isolated in 1991, fifteen homologues have been reported to date.<sup>1–7</sup> Among those, AM3 significantly exceeds other homologues in the antifungal activity. The absolute configuration of AM3 (Fig. 1) was determined by extensive NMR experiments such as the *J*-based configuration analysis (JBCA) method, modified Mosher method, and HPLC analysis of the degradation products.<sup>15</sup> Recently, we have revised the stereochemistry of C2 of AM3 to be *R* by comparing synthetic specimens with a fragment of AM3 and by GC–MS.<sup>16</sup>

We have previously<sup>3,4,17</sup> revealed that AMs increase membrane permeability by directly interacting with lipid bilayers. The distinct partition coefficients ( $K'_m$  values) to multilamellar vesicle (MLV) membrane were examined by HPLC quantification for AMs<sup>17</sup>; the  $K'_m$  values of AM2, AM3, and AM4 in eggPC preparations were  $0.77 \times 10^3$ ,  $22.2 \times 10^3$  and  $2.24 \times 10^3$ , respectively. The order in

$K'_m$  values agrees well with those of the membrane-permeabilizing and antifungal activities, where AM3 with a butadiene terminus binds most efficiently to PC membrane.

Permeabilization of the phospholipid membrane by AMs is thought to be responsible for their potent antifungal activity. Moreover, AMs permeabilize the membrane more efficiently in the presence of sterol.<sup>3,4,17–19</sup> The size of the pore/lesion formed in the erythrocyte membrane was estimated to be 2.0–2.9 nm in diameter which was significantly larger than those of other antifungals such as amphotericin B (AmB).<sup>18</sup> Structure–activity relationship<sup>7</sup> using naturally occurring AMs and chemically modified AM derivatives has showed that the polyene and polyhydroxy moieties play respective roles in binding to the lipid bilayer membrane and in forming an ion-permeable pore/lesion across the membrane. In order to gain insight into the membrane-bound structure of AMs, conformational analysis of AM3 has been carried out on the basis of high-resolution <sup>1</sup>H NMR data measured for SDS micelles<sup>17</sup> and isotropic bicelles.<sup>20</sup> These experiments have revealed that the central region of AM3 takes a hairpin conformation while the hydrophobic polyene chain is immersed in the hydrophobic interior. The efficacies of AM2 and AM3 have been measured by fluorescent-dye leakage experiments for POPC liposomes with various cholesterol and ergosterol contents, indicating that, with increasing concentrations of the sterol, the membrane permeability are increased significantly.<sup>19</sup> Moreover, cholesterol and ergosterol have a similar efficacy in enhancement of the AM activities.

By using surface plasmon resonance (SPR) techniques, which are shown to be useful for membrane-bound peptides and drugs,<sup>21–23</sup> we successfully evaluated interaction between AmB and lipid bilayers.<sup>24</sup> To examine more closely the affinity of AM3 to membranes

<sup>\*</sup> Corresponding author.

E-mail address: [murata@ch.wani.osaka-u.ac.jp](mailto:murata@ch.wani.osaka-u.ac.jp) (M. Murata).

<sup>†</sup> Present address: Department of Chemistry of Natural Compounds, National Research Centre, Dokki, Cairo, Egypt.

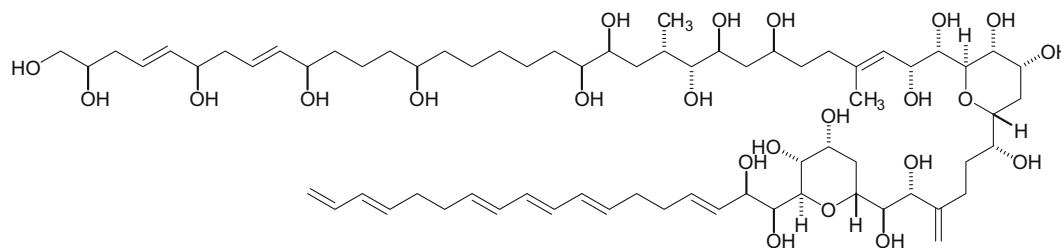


Figure 1. Amphidinol 3 (AM3).

with or without sterol in this study, we utilized the same dodecylamine-modified SPR sensor chip<sup>24</sup> to carry out kinetic analysis for AM3 binding to sterol-containing and sterol-free palmitoyl-oleoyl-phosphatidylcholine (POPC) liposomes.

Amphidinol 3 was isolated from the marine dinoflagellate *Amphidinium klebsii* (deposited in National Institute for Environmental Studies as NIES 613) as described previously.<sup>5</sup> Briefly, the unialgal culture was grown in artificial seawater enriched with ES-1 supplement at 25 °C under illumination of a 16–8 light–dark photocycle for 4 weeks. Harvested cells were extracted and treated with an ODS open column and HPLC. Liposomes used in the experiments were prepared by evaporating sterol-containing or sterol-free POPC solution to form dry film, which was then suspended in PBS buffer, frozen and thawed, vortexed and finally extruded through polycarbonated membrane to predominantly yield large unilamellar vesicles with 100 nm in diameter. Details of experimental methods are described in [Supplementary data](#).<sup>28</sup>

The CM5 chip of SPR was modified with dodecylamine to prepare a hydrophobic surface. One of two flow cell lanes in the CM5 chip was modified with dodecylamine, while the other lane remained intact for the use of a control run.<sup>28</sup> To the modified lane, POPC and POPC/sterol liposomes were stably captured. When the liposomes at the phospholipid concentration of 0.5 mM were introduced, the SPR response due to liposome association reached about 10,000 RU (Fig. 2). The sensor chip was tolerant of NaOH treatments (50 mM), and the amount of captured liposomes was essentially unchanged by repetitive washing. For kinetic analysis, the binding of AM3 to liposome membranes was standardized as an amount of AM3 in RU bound to the amount of lipids equivalent to 10,000 RU.

Detection of AM3 affinity was carried out in PBS buffer (pH 7.4) as running and injection media. AM3 dissolved in PBS buffer was

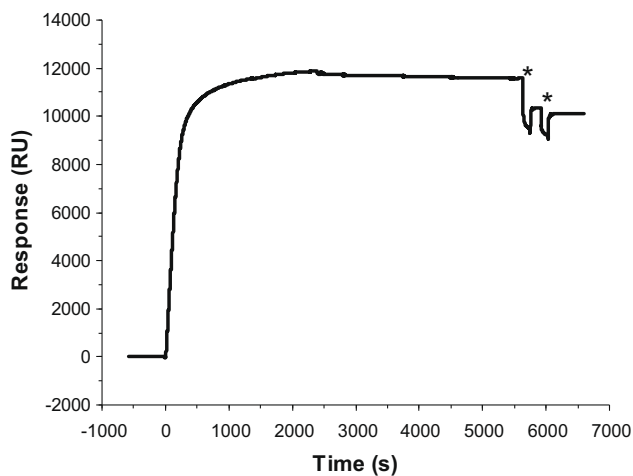


Figure 2. Immobilization of 0.5 mM POPC liposome (80  $\mu$ L) on dodecylamine-modified CM5 sensor chip. Liposome-bound surface was washed twice with 50 mM NaOH for 2 min at 20  $\mu$ L/min (denoted by asterisks).

then passed on the sensor chip treated with liposomes. The SPR response increased immediately after injection due to interaction between AM3 in the sample solution and POPC liposomes immobilized on the surface of the sensor chip. To evaluate AM3 binding to sterol-containing or sterol-free liposomes, the SPR response in the control lane was subtracted from that in the liposome-captured lane.<sup>28</sup> AM3 firmly interacted with the sensor-chip surface and a small portion of AM3 was hardly washed out during regeneration. To eliminate the effect of the remaining AM3, we always used a newly prepared sensor chip.

Typical sensorgrams for interaction of 10  $\mu$ M AM3 with 5% cholesterol-containing POPC liposomes and sterol-free ones were shown in Figure 3. The RU changes upon AM3 addition are largely responsible for the drug-liposome interaction. As is evident from Figure 3, AM3 bound preferentially to cholesterol-containing liposomes. We next carried out kinetic analysis of the drug's binding to membrane using BIA evaluation software for the reaction models including Langmuir binding, bivalent analyte, and two-state reaction models. Among those, the two-state reaction model best reproduced the experimental sensorgrams as depicted in Figure 3.

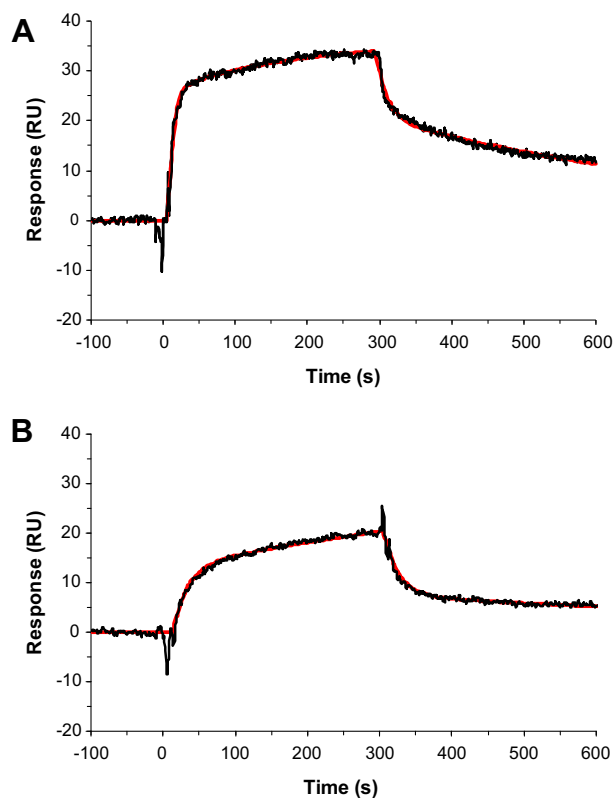


Figure 3. Typical sensorgrams for interaction of 10  $\mu$ M AM3 to 5% cholesterol-containing POPC (A) and to sterol-free POPC (B). The sensorgrams were fitted to the two-state reaction model (smooth red lines).

The two-state reaction model indicates that the interaction is composed of subsequent two steps; the first step is partition of AM3 to the POPC phase of liposomes, and the second step probably corresponds to the internalization of AM3 to the liposome interior to form more stable complexes.

Then, we estimated the kinetic parameters of AM3 binding to the membranes based on the two-state reaction model<sup>23</sup> as presented in Table 1. In this model,  $k_{a1}$  and  $k_{d1}$  are association and dissociation constants of analyte to membrane surface in the first step while  $k_{a2}$  and  $k_{d2}$  are association and dissociation rates for the second step. Then  $K_{A1}$ ,  $K_{A2}$  and  $K_A$  represent the affinity constants for the first step, the second step and overall equilibrium, respectively, and were calculated from the association and dissociation rate constants<sup>29</sup> (see Supplementary data for details).

As depicted in Figure 4, sterols have the most striking effects on the initial process of AM3 binding to membrane as revealed by  $k_{a1}$ . The  $k_{a1}$  value of AM3 in 5% cholesterol- and ergosterol-containing membranes exceeds that in the sterol-free membranes by about 180- and 35-fold, respectively. This suggests that sterols play a functional role in capturing AM3 on the membrane surface. The resultant  $K_A$  value of AM3 in 5% cholesterol-containing membrane exceeds that in the sterol-free one by almost 1000-fold. The binding step to membrane is, as aforementioned, one of important features for the biological activity.<sup>17</sup> Although effect of ergosterol on the initial binding process is not as dramatic as that of cholesterol, ergosterol stabilizes formation of complex in the second step. As a result, the  $K_A$  value of AM3 in 5% ergosterol-containing membrane exceeds that in the sterol-free one by about 5000-fold.

The binding of AM3 to the POPC liposomal membrane is very strong. It was therefore extremely difficult to regenerate the membrane once AM3 bound to it. We had to prepare the new liposome surface on the sensor chip each time to replicate the experiments. As a result, similar membrane conditions were not attainable for each run, which caused relatively large standard error means in Table 1. Nonetheless, large differences between kinetic constants obtained in the presence and absence of sterols clearly indicate that sterols markedly enhance the membrane-binding of AM3.

**Table 1**

Kinetic and affinity constants for interactions of AM3 (10  $\mu$ M) with POPC liposomes in the presence and absence of 5% sterol estimated from the two-state reaction model

Kinetic value	POPC + Erg	POPC + Cho	POPC
$k_{a1}$ ( $\times 10^3$ /Ms)	$1.64 \pm 0.43$	$8.53 \pm 0.61$	$0.0465 \pm 0.0057$
$k_{d1}$ ( $\times 10^{-3}$ /s)	$12.5 \pm 2.8$	$48.0 \pm 6.2$	$51.9 \pm 3.1$
$k_{a2}$ ( $\times 10^{-3}$ /s)	$12.4 \pm 3.2$	$7.65 \pm 1.27$	$2.62 \pm 0.23$
$k_{d2}$ ( $\times 10^{-3}$ /s)	$0.420 \pm 0.070$	$1.98 \pm 0.13$	$3.96 \pm 1.52$
$K_{A1}$ ( $\times 10^3$ /M)	$143 \pm 23$	$180 \pm 11$	$0.901 \pm 0.121$
$K_{A2}$	$28.6 \pm 2.62$	$3.92 \pm 0.71$	$0.930 \pm 0.380$
$K_A$ ( $\times 10^3$ /M)	$3970 \pm 410$	$721 \pm 169$	$0.764 \pm 0.226$

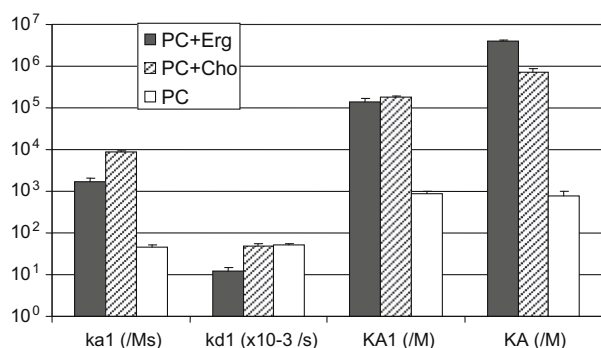


**Figure 4.** Comparison kinetic data in logarithmic scale for AM3 binding to ergosterol-, cholesterol-containing and sterol-free POPC liposomes.

These effects of cholesterol, mammalian sterol, and ergosterol, fungal sterol<sup>25</sup> may account for the respective potent cytotoxicity<sup>6,26</sup> and antifungal activities.<sup>1–7</sup> Interestingly, AMs lack anti-bacterial activity, which is probably due to the absence of sterols in bacterial membranes. Moreover, AM3 showed higher affinity to ergosterol membrane than cholesterol one, particularly, in dissociation process;  $K_{A2}$  of the former was significantly larger than those of the latter. These observations indicate that AM3 forms more stable complex in the presence of ergosterol and may provide a clue for developing a new antifungal drug.

In conclusion, we disclosed that sterols markedly enhance affinity of AM3 to phospholipid membrane. The present results support previous findings in fluorescent-dye leakage experiments,<sup>19</sup> the potentiation of the activity of AM3 by sterol is prominent even at 0.5% (w/w) to the lipid, which ruled out the possibility that alteration of the membrane physical properties elicited by sterols<sup>27</sup> was responsible for this effect.<sup>19</sup> The significantly larger  $K_{A2}$  for POPC-ergosterol membrane (Table 1) further supports the notion that sterols, particularly ergosterol, not only accelerate partition of AM3 to membrane but also stabilize the membrane-bound complex formed by AM3, suggesting the direct interaction between AM3 and sterols in the complex. NMR-based investigations on this interaction in membrane model systems are now in progress in our laboratory.

## Acknowledgements

This work was supported by Grants-in-Aid for Scientific Research (S) (No. 18101010), for Priority Area (A) (No. 16073211), and for Young Scientists (A) (No. 17681027) from MEXT, Japan as well as by The Naito Foundation. A Monbukagakusho scholarship to R.T.S. is also greatly acknowledged.

## Supplementary data

Supplementary data associated with this article can be found, in the online version, at [doi:10.1016/j.bmcl.2010.02.025](https://doi.org/10.1016/j.bmcl.2010.02.025).

## References and notes

- Satake, M.; Murata, M.; Yasumoto, T.; Fujita, T.; Naoki, H. *J. Am. Chem. Soc.* **1991**, *113*, 9859.
- Paul, G. K.; Matsumori, N.; Murata, M.; Tachibana, K. *Tetrahedron Lett.* **1995**, *36*, 6279.
- Paul, G. K.; Matsumori, N.; Konoki, K.; Sasaki, M.; Murata, M.; Tachibana, K. In *Harmful and Toxic Algal Blooms*, Sendai, July, 1995; Intergovernmental Oceanographic Commission of UNESCO: Sendai, 1995; 503.
- Paul, G. K.; Matsumori, N.; Konoki, K.; Murata, M.; Tachibana, K. *J. Mar. Biotechnol.* **1997**, *5*, 124.
- Morsy, N.; Matsuoka, S.; Houdai, T.; Matsumori, N.; Adachi, S.; Murata, M.; Iwashita, T.; Fujita, T. *Tetrahedron* **2005**, *61*, 8606.
- Echigoya, R.; Rhodes, L.; Oshima, Y.; Satake, M. *Harmful Algae* **2005**, *4*, 383.
- Morsy, N.; Houdai, T.; Matsuoka, S.; Matsumori, N.; Adachi, S.; Oishi, T.; Murata, M.; Iwashita, T.; Fujita, T. *Bioorg. Med. Chem.* **2006**, *14*, 6548.
- Doi, Y.; Ishibashi, M.; Nakamichi, H.; Kosaka, T.; Ishikawa, T.; Kobayashi, J. *J. Org. Chem.* **1997**, *62*, 3820.
- Kubota, T.; Tsuda, M.; Doi, Y.; Takahashi, A.; Nakamichi, H.; Ishibashi, M.; Fukushima, E.; Kawabata, J.; Kobayashi, J. *Tetrahedron* **1998**, *54*, 14455.
- Kubota, T.; Takahashi, A.; Tsuda, M.; Kobayashi, J. *Mar. Drugs* **2005**, *3*, 113.
- Huang, X.-C.; Zhao, D.; Guo, Y.-W.; Wu, H.-M.; Trivellone, E.; Cimino, G. *Tetrahedron Lett.* **2004**, *45*, 5501.
- Washida, K.; Koyama, T.; Yamada, K.; Kita, M.; Uemura, D. *Tetrahedron Lett.* **2006**, *47*, 2521.
- Kubota, T.; Sakuma, Y.; Shimbo, K.; Tsuda, M.; Nakano, M.; Uozumi, Y.; Kobayashi, J. *Tetrahedron Lett.* **2006**, *47*, 4369.
- Huang, S.-J.; Kuo, C.-M.; Lin, Y.-C.; Chen, Y.-M.; Lu, C.-K. *Tetrahedron Lett.* **2009**, *50*, 2512.
- Murata, M.; Matsuoka, S.; Matsumori, N.; Paul, G. K.; Tachibana, K. *J. Am. Chem. Soc.* **1999**, *121*, 870.
- Oishi, T.; Kanemoto, M.; Swasono, R.; Matsumori, N.; Murata, M. *Org. Lett.* **2008**, *10*, 5203.
- Houdai, T.; Matsuoka, S.; Morsy, N.; Matsumori, N.; Satake, M.; Murata, M. *Tetrahedron* **2005**, *61*, 2795.

18. Houdai, T.; Matsuoka, S.; Matsumori, N.; Murata, M. *Biochim. Biophys. Acta* **2004**, 1667, 91.
19. Morsy, N.; Houdai, T.; Konoki, K.; Matsumori, N.; Oishi, T.; Murata, M. *Bioorg. Med. Chem.* **2008**, 16, 3084.
20. Houdai, T.; Matsumori, N.; Murata, M. *Org. Lett.* **2008**, 10, 4191.
21. Abdiche, Y. N.; Myszk, D. G. *Anal. Biochem.* **2004**, 328, 233.
22. Papo, N.; Shai, Y. *Biochemistry* **2003**, 42, 458.
23. Mozzolits, H.; Wirth, H. J.; Werkmeister, J.; Aguilar, M. I. *Biochim. Biophys. Acta* **2001**, 1512, 64.
24. Mouri, R.; Konoki, K.; Matsuoka, S.; Oishi, T.; Murata, M. *Biochemistry* **2008**, 47, 7807.
25. Bolard, J. *Biochim. Biophys. Acta* **1986**, 864, 257.
26. Qi, X.-M.; Yu, B.; Huang, X.-C.; Guo, Y.-W.; Zhai, Q.; Jin, R. *Toxicol.* **2007**, 50, 278.
27. Alvarez, F. J.; Douglas, L. M.; Konopka, J. B. *Eukaryot. Cell* **2007**, 6, 755.
28. [Supplementary data](#) is available on the online version
29. The association rate constants ( $k_{a1}$  and  $k_{a2}$ ), the dissociation rate constants ( $k_{d1}$  and  $k_{d2}$ ) and the equilibration constants  $K_{A1}$  ( $k_{a1}/k_{d1}$ ),  $K_{A2}$  ( $k_{a2}/k_{d2}$ ) and  $K_A$  ( $k_{a1}/k_{d1} \times k_{a2}/k_{d2}$ ).